Supporting Information

Atomically dispersed Pt catalyst on ceria-carbon to suppress C-C cleavage in glycerol electrooxidation

Hae Ryeong Lee†, Eunchong Lee†, Yunji Choi, Jaehoon Kwon, Seonmin Jeon, Sujin Park, Yun Jeong Hwang, Hyunjoo Lee**

Additional Data; Figure S1 ~ S23, Table S1 ~ S6

† These authors contributed equally.

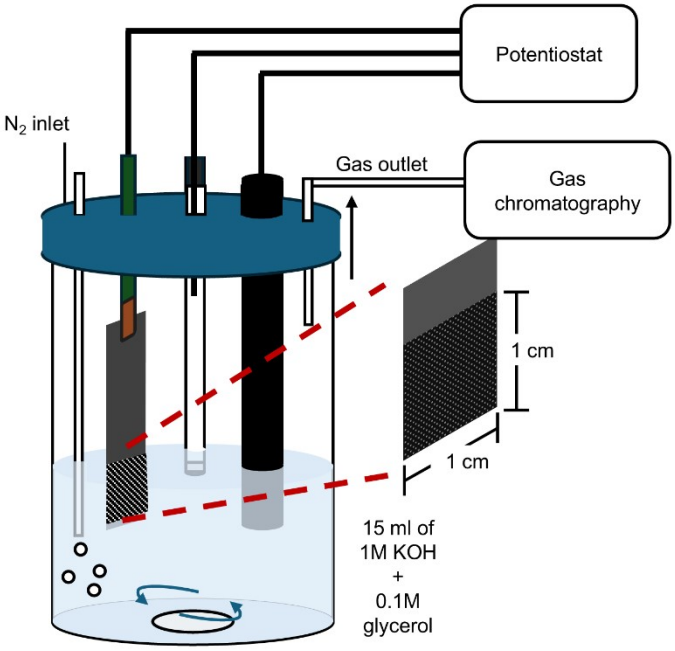

Figure S1. Schematic diagram of the batch system used for glycerol electrooxidation.

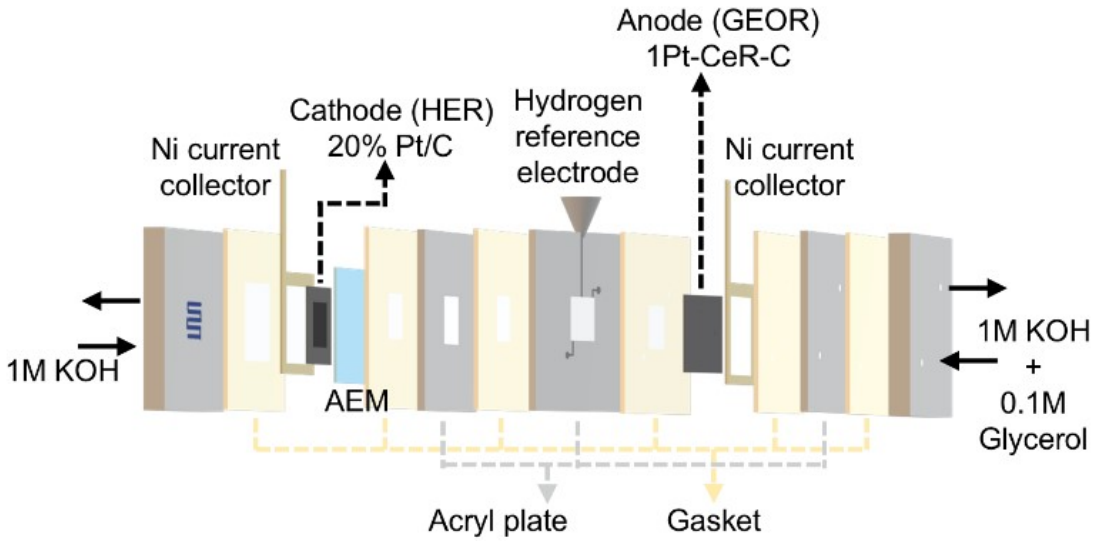

Figure S2. Detailed schematic diagram of the flow cell

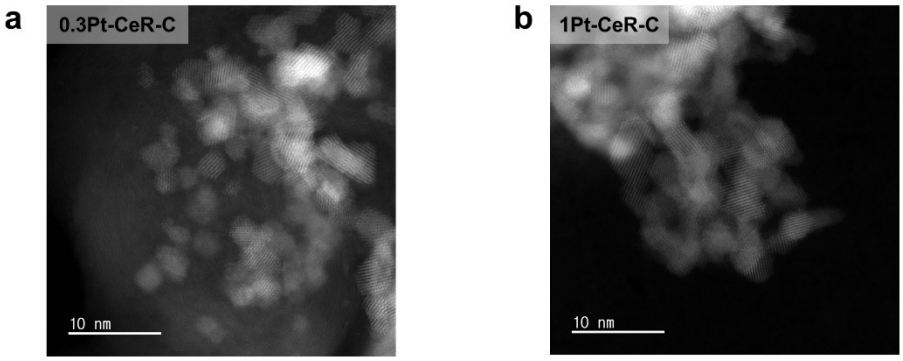

Figure S3. No Pt clusters found in 0.3Pt-CeR-C and 1Pt-CeR-C. HAADF-STEM images of a) 0.3Pt-CeR-C and b) 1Pt-CeR-C.

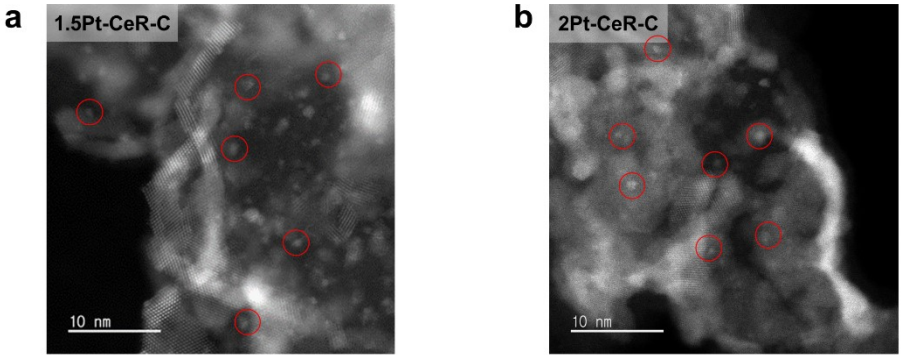

Figure S4. HAADF-STEM images of a) 1.5Pt-CeR-C and b) 2Pt-CeR-C.

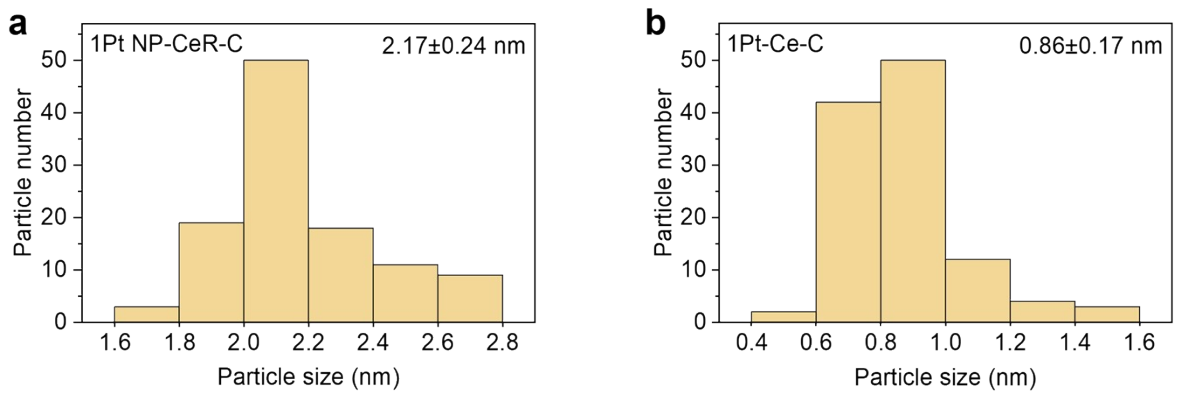

Figure S5. Size distribution of Pt nanoparticles for a) 1Pt NP-CeR-C and b) 1Pt-Ce-C, based on HAADF-STEM images.

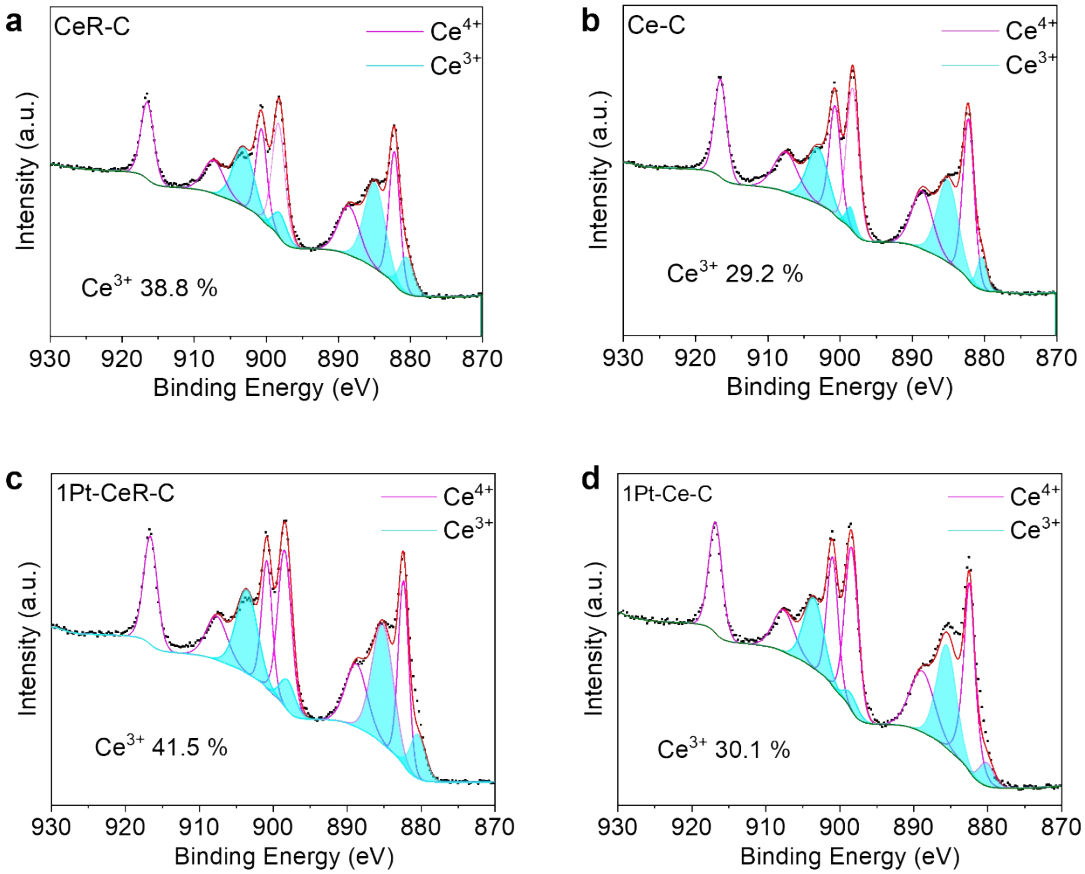

Figure S6. Ce 3d XPS spectra of a) CeR-C, b) Ce-C, c) 1Pt-CeR-C, and d) 1Pt-Ce-C.

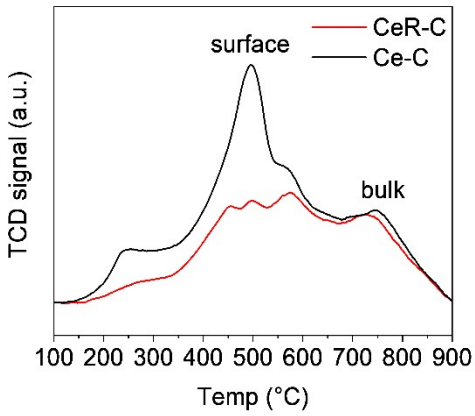

Figure S7. H_2-TPR profiles of CeR-C and Ce-C supports.

Table S1. Fitting parameters and results of EXAFS analysis of all samples and Pt foil.

Sample	Shell	CN	R (A)	$\sigma^2 \cdot 10^{-3}$ ($Å^2$)	R factor
0.3Pt-CeR-C	Pt-Cl	3.8 ± 0.5	2.02 ± 0.02	6.0 ± 1.3	0.018
	Pt-Pt	0.6 ± 0.2	2.67 ± 0.06	2.2 ± 1.6	
1Pt-CeR-C	Pt-Cl	3.5 ± 0.5	2.28 ± 0.02	8.9 ± 1.3	0.030
	Pt-Pt	0.8 ± 0.3	2.77 ± 0.07	6.0 ± 2.3	
1Pt NP-CeR-C	Pt-Cl	0.6 ± 0.1	2.21 ± 0.09	1.6 ± 0.8	0.054
	Pt-Pt	8.9 ± 0.4	2.76 ± 0.09	7.8 ± 2.5	
1Pt-Ce-C	Pt-Cl	2.9 ± 0.5	2.17 ± 0.02	3.8 ± 0.5	0.014
	Pt-Pt	1.4 ± 0.3	2.84 ± 0.06	2.5 ± 1.0	
Pt foil	Pt-Pt	12	2.76 ± 0.02	4.9 ± 0.4	0.024

CN: coordination number; R: bond distance; σ^2: Debye-Waller factors

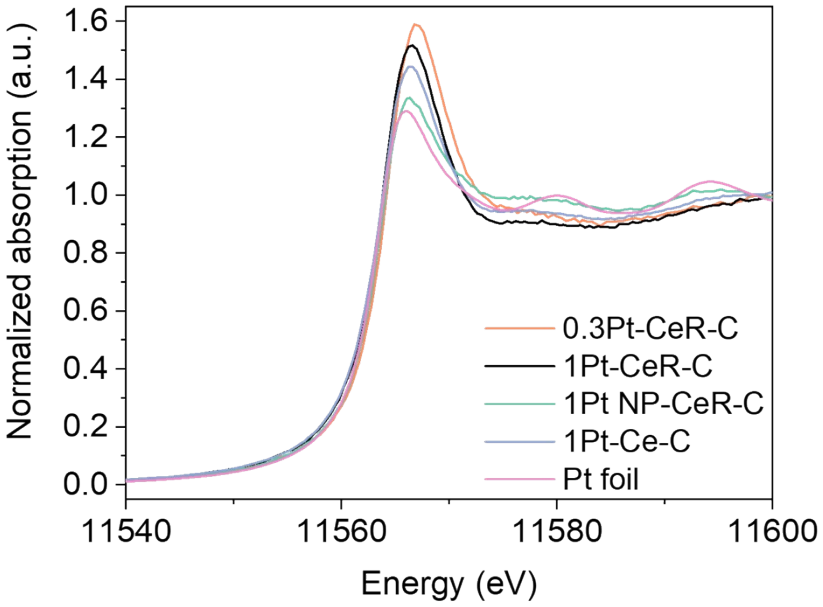

Figure S8. XANES results of all the Pt-based catalysts.

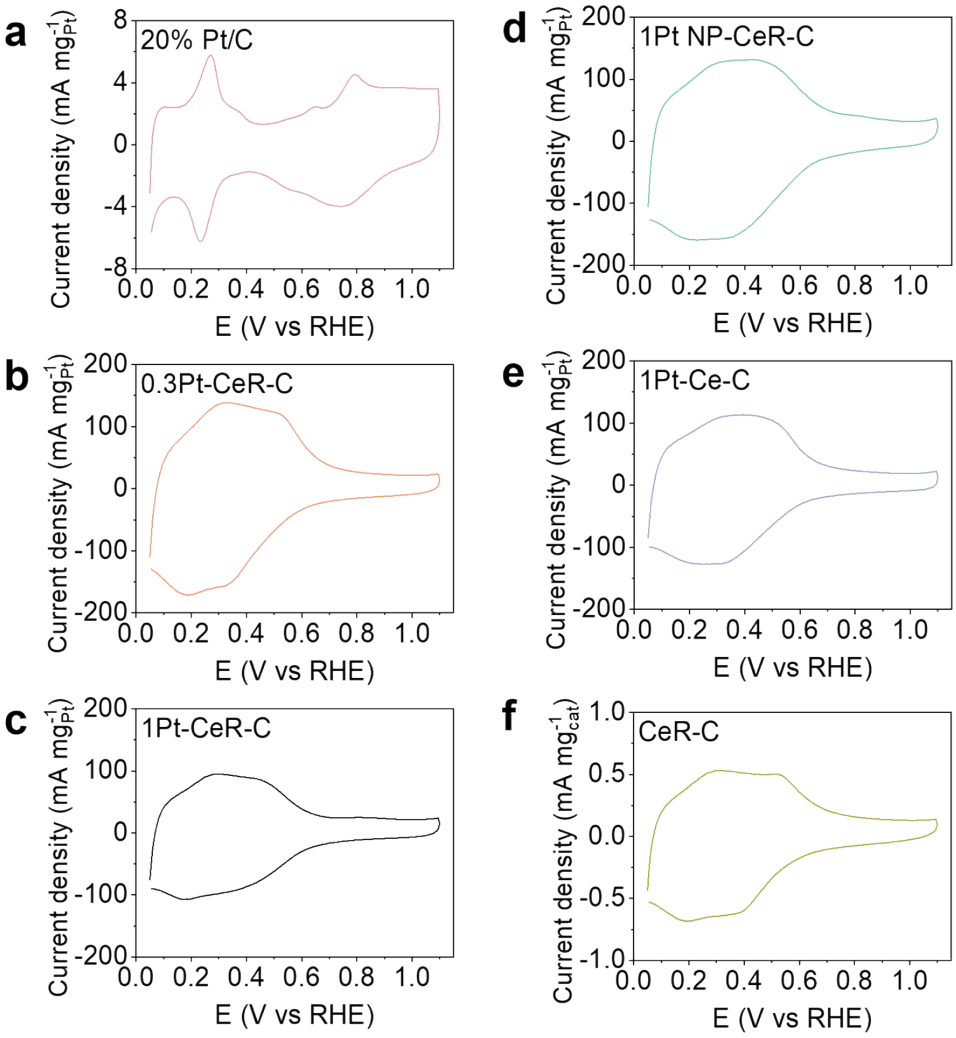

Figure S9. CV profiles in 1 M KOH for a) 20% Pt/C, b) 0.3Pt-CeR-C, c) 1Pt-CeR-C, d) 1Pt NP-CeR-C, e) 1Pt-Ce-C, e), and f) CeR-C. The scan rate was 10 mV s^{-1}.

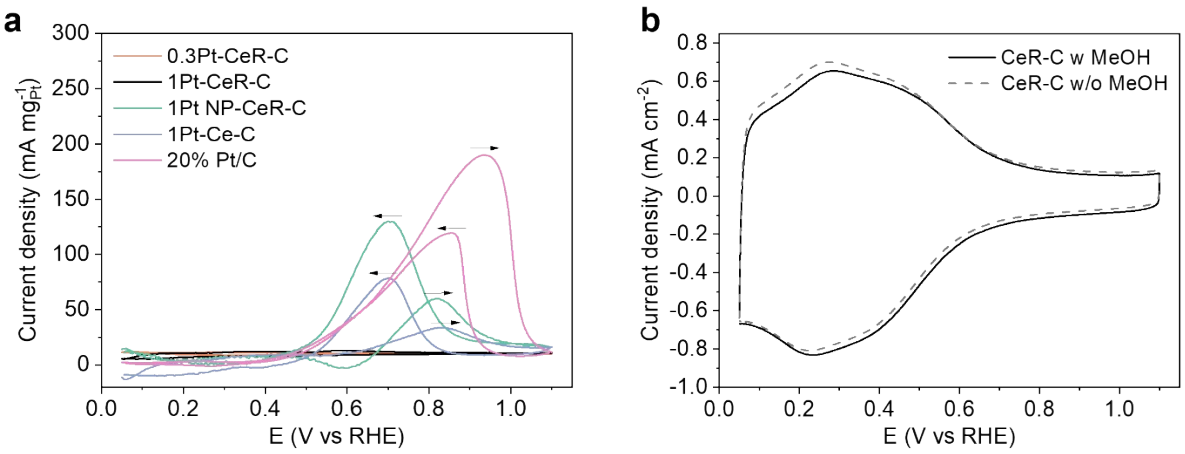

Figure S10. CV profiles of a) various Pt catalysts in an aqueous solution of 1 M KOH + 0.5 M MeOH and b) CeR-C support in an aqueous solution of 1 M KOH with or without 0.5 M MeOH. The scan rate was 10 mV s^{-1}. The forward and backward scans were denoted with the arrows in (a).

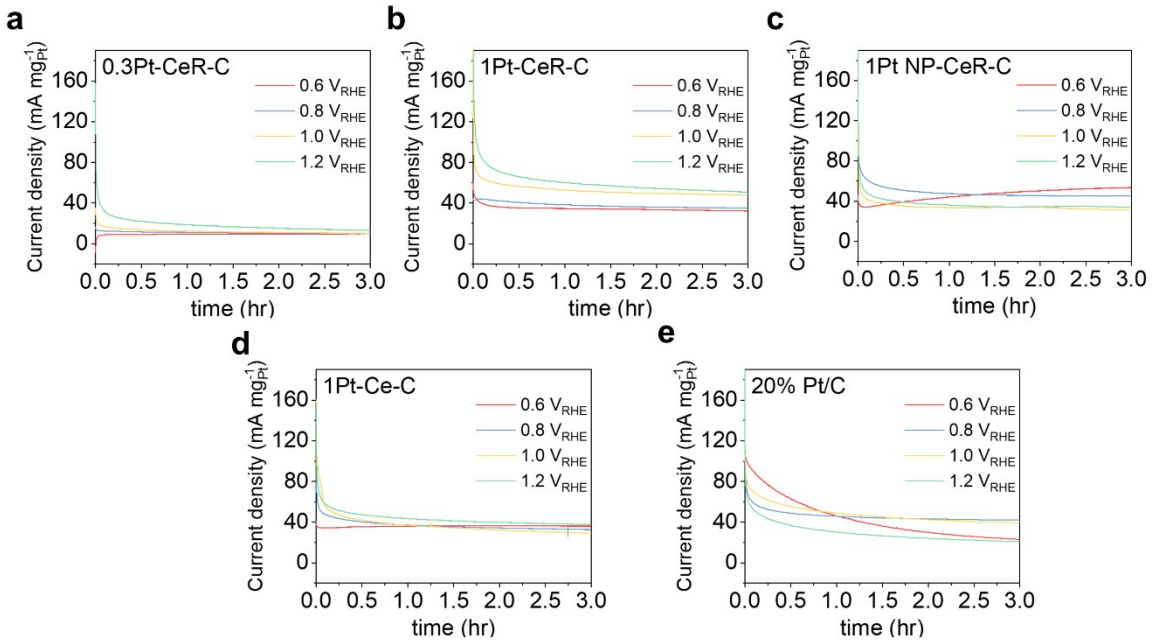

Figure S11. Chronoamperometric curve under 0.6 V_{RHE}, 0.8 V_{RHE}, 1.0 V_{RHE}, and 1.2 V_{RHE} for 3 hrs for a) 0.3Pt-CeR-C, b) 1Pt-CeR-C, c) 1Pt NP-CeR-C, d) 1Pt-Ce-C, and e) 20% Pt/C. The currents were normalized by Pt mass loading.

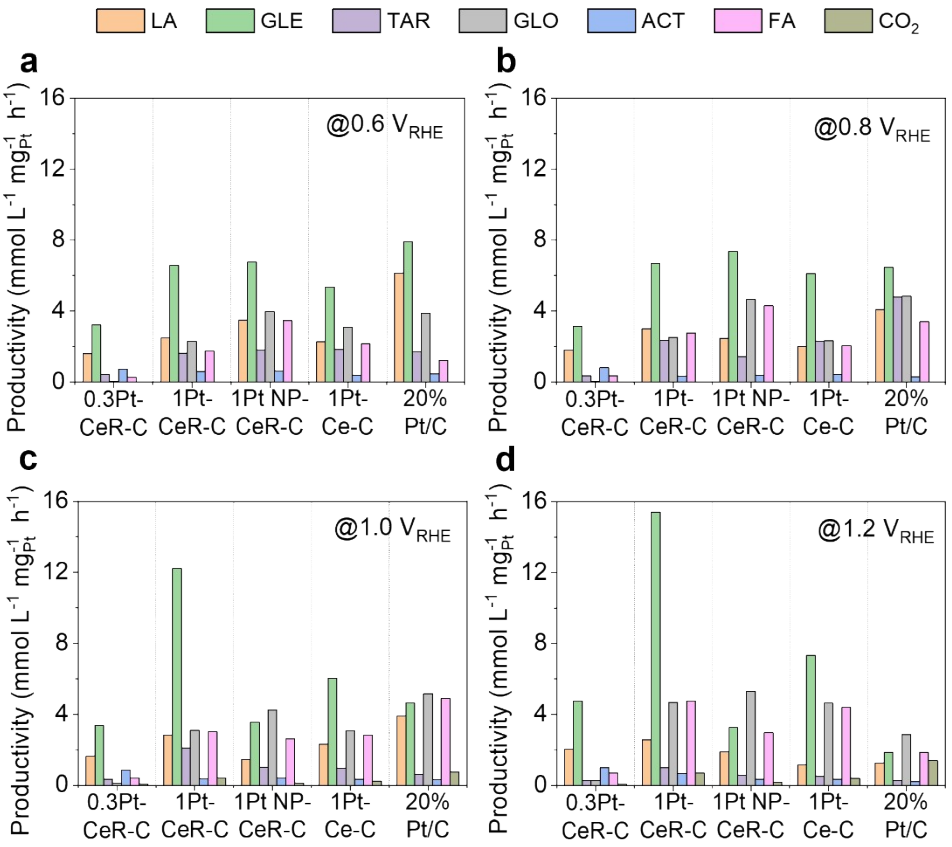

Figure S12. The productivities of each GEOR product after 3hrs of electrooxidation at a) 0.6 V_{RHE}, b) 0.8 V_{RHE}, c) 1.0 V_{RHE}, and d) 1.2 V_{RHE}, performed in 1 M KOH + 0.1 M glycerol. LA lactate; GLE glycerate; TAR tartronate; GLO glycolate; ACT acetate; FA formate.

Table S2. GEOR productivity, selectivity, glycerol conversion (η_{gly}), and total faradaic efficiency (FE) for every catalyst in an electrolyte of 1 M KOH + 0.1 M glycerol at different potentials.

Catalyst	Potential (V_{RHE})	Productivity (mmol L^{-1} mg_{PGM}^{-1} h^{-1}) (Selectivity (%))							η_{gly}[a] (%)	FE (%)
		LA	GLE	TAR	GLO	ACT	FA	CO_2		
0.3Pt-CeR-C	0.6	1.61 (25.6)	3.22 (51.2)	0.42 (6.7)	0.03 (0.5)	0.74 (11.8)	0.27 (4.3)	- -	6.6	99.1
	0.8	1.81 (27.8)	3.14 (48.3)	0.35 (5.4)	0.04 (0.6)	0.81 (12.5)	0.35 (5.4)	- -	9.6	87.2
	1.0	1.64 (24.1)	3.36 (49.3)	0.33 (4.8)	0.13 (1.9)	0.87 (12.8)	0.41 (6.0)	0.07 (1.0)	4.2	85.1
	1.2	2.06 (22.5)	4.76 (52.1)	0.26 (2.8)	0.28 (3.1)	1.00 (10.9)	0.70 (7.7)	0.08 (0.9)	10.1	76.3
1Pt-CeR-C	0.6	2.48 (16.2)	6.58 (43.0)	1.62 (10.6)	2.30 (15.0)	0.59 (3.9)	1.75 (11.4)	- -	13.6	82.7
	0.8	3.01 (17.0)	6.69 (37.9)	2.34 (13.3)	2.53 (14.3)	0.33 (1.9)	2.76 (15.6)	- -	15.3	92.1
	1.0	2.84 (11.8)	12.22 (50.8)	2.11 (8.8)	3.10 (12.9)	0.37 (1.5)	3.01 (12.5)	0.41 (1.7)	16.5	89.3
	1.2	2.56 (8.6)	15.39 (51.6)	1.00 (3.4)	4.69 (15.7)	0.69 (2.3)	4.77 (16.0)	0.70 (2.3)	19.0	98.8
1Pt NP-CeR-C	0.6	3.49 (17.3)	6.76 (33.6)	1.82 (9.0)	3.97 (19.7)	0.62 (3.1)	3.46 (17.2)	- -	16.9	84.4
	0.8	2.47 (12.0)	7.36 (35.8)	1.42 (6.9)	4.65 (22.6)	0.39 (1.9)	4.29 (20.8)	- -	20.7	86.8
	1.0	1.45 (10.8)	3.56 (26.5)	1.01 (7.5)	4.24 (31.6)	0.41 (3.1)	2.62 (19.5)	0.13 (1.0)	14.9	81.8
	1.2	1.88 (12.9)	3.27 (22.5)	0.57 (3.9)	5.29 (36.4)	0.36 (2.5)	2.97 (20.4)	0.20 (1.4)	14.7	81.6
1Pt-Ce-C	0.6	2.27 (15.0)	5.36 (35.5)	1.84 (12.2)	3.08 (20.4)	0.39 (2.6)	2.15 (14.2)	- -	13.0	82.7
	0.8	2.00 (13.1)	6.12 (40.1)	2.31 (15.1)	2.33 (15.3)	0.44 (2.9)	2.05 (13.4)	- -	11.7	82.4
	1.0	2.31 (14.6)	6.03 (38.2)	0.97 (6.1)	3.08 (19.5)	0.34 (2.2)	2.83 (17.9)	0.22 (1.4)	14.8	85.1
	1.2	1.16 (6.2)	7.34 (39.0)	0.53 (2.8)	4.65 (24.7)	0.36 (1.9)	4.40 (23.4)	0.40 (2.1)	15.6	93.5
Pt/C	0.6	6.14 (28.8)	7.92 (37.1)	1.71 (8.0)	3.88 (18.2)	0.47 (2.2)	1.22 (5.7)	- -	17.0	82.0
	0.8	4.10 (17.1)	6.47 (27.1)	4.79 (20.0)	4.84 (20.2)	0.31 (1.3)	3.40 (14.2)	- -	18.8	108.8
	1.0	3.92 (19.3)	4.64 (22.8)	0.62 (3.1)	5.17 (25.5)	0.32 (1.6)	4.89 (24.1)	0.75 (3.7)	14.2	90.0
	1.2	1.26 (12.9)	1.86 (19.1)	0.27 (2.8)	2.87 (29.5)	0.21 (2.2)	1.86 (19.1)	1.40 (14.4)	11.4	82.7

[a] $\eta_{gly}\,(\%) = \frac{conc_{initial\ glycerol} - conc_{final\ glycerol}}{conc_{initial\ glycerol}} \times 100\%$

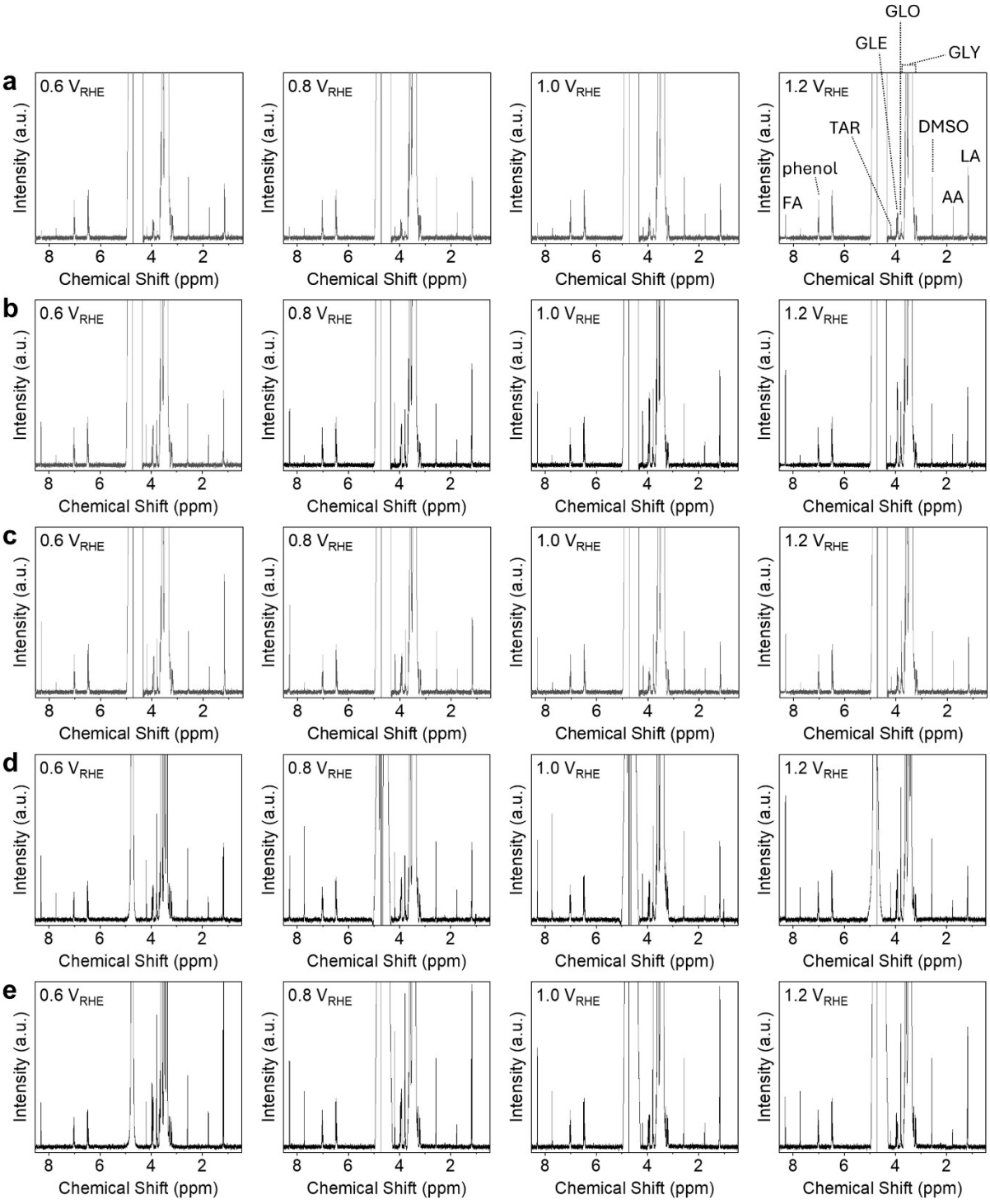

Figure S13. NMR result of a) 0.3Pt-CeR-C, b) 1Pt-CeR-C, c) 1Pt NP-CeR-C, d) 1Pt-Ce-C and e) 20% Pt/C after GEOR at each applied potentials for 3 hrs.

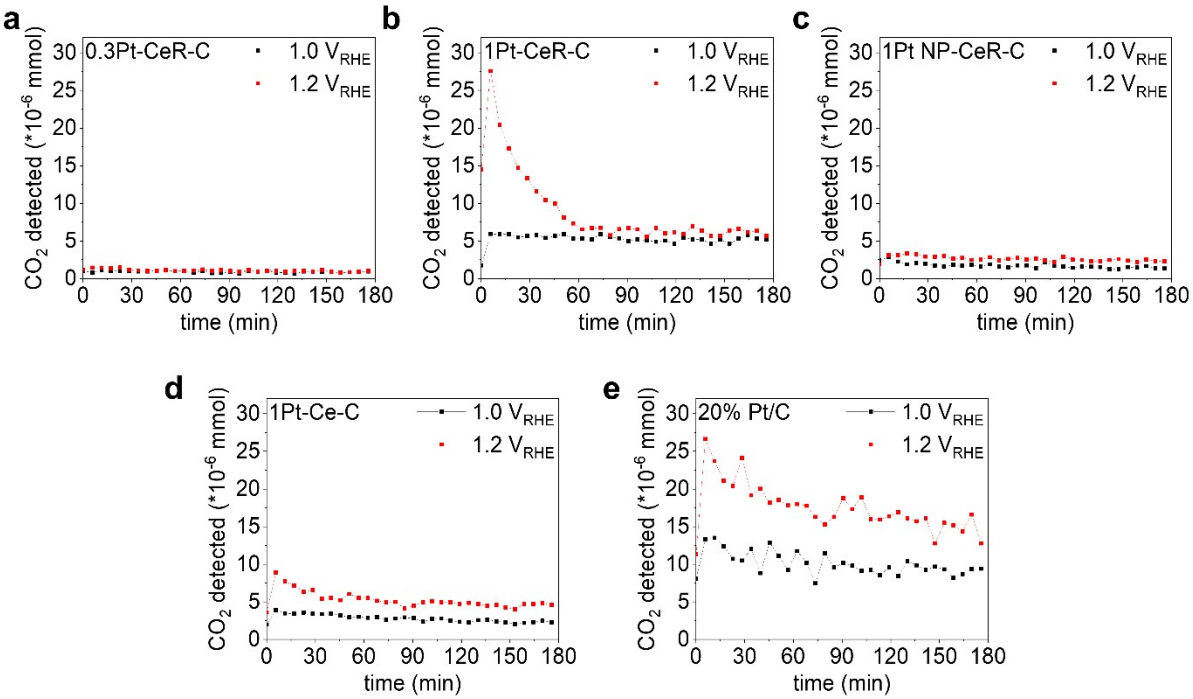

Figure S14. GC result of a) 0.3Pt-CeR-C, b) 1Pt-CeR-C, c) 1Pt NP-CeR-C, d) 1Pt-Ce-C and e) 20% Pt/C during GEOR at each applied potential for 3 hrs.

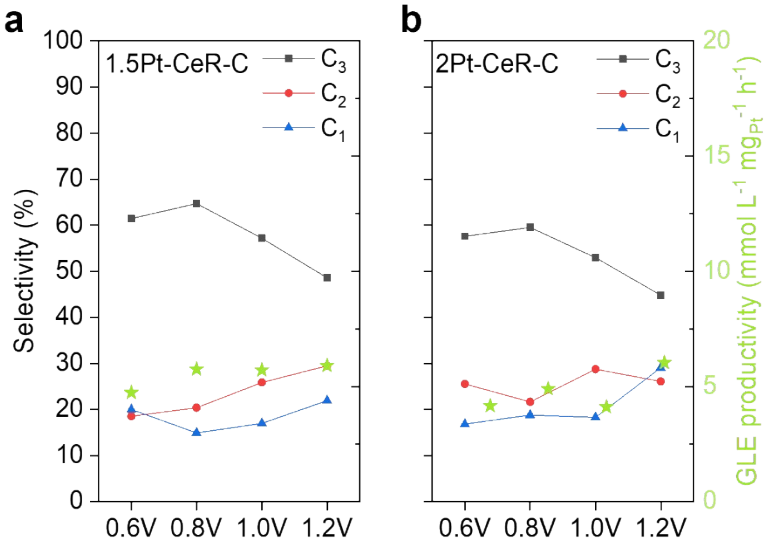

Figure S15. The selectivity of C_3, C_2 and C_1 and the GLE productivity at each potential (vs RHE) for a) 1.5Pt-CeR-C and b) 2Pt-CeR-C.

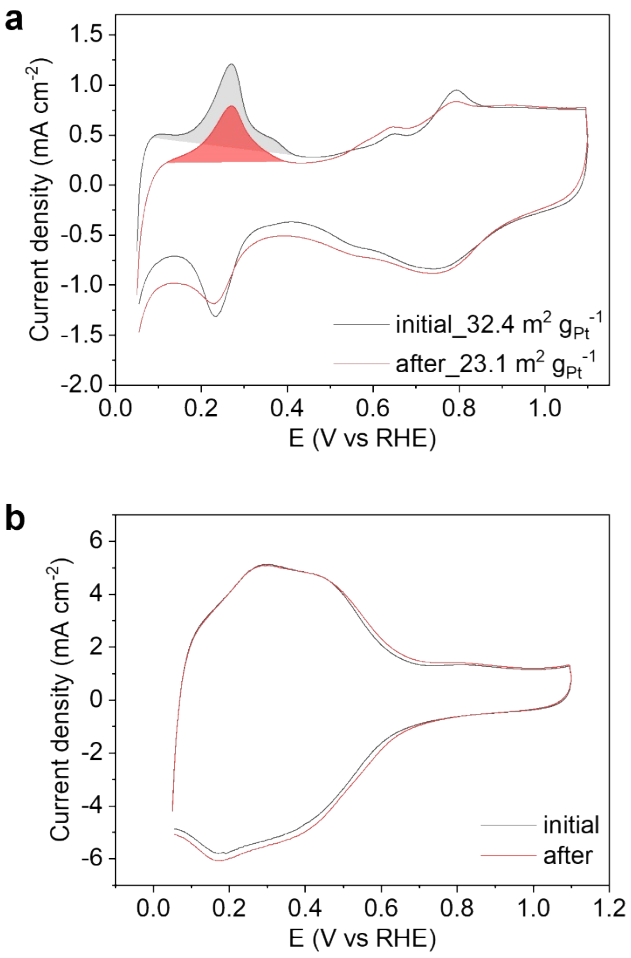

Figure S16. CV profiles of a) 20% Pt/C and b) 1Pt-CeR-C in 1 M KOH before and after GEOR at 1.2 V_{RHE} for 3 hrs. The scan rate was 10 mV s^{-1}. The shaded areas were used to calculate the ECSA of Pt in (a).

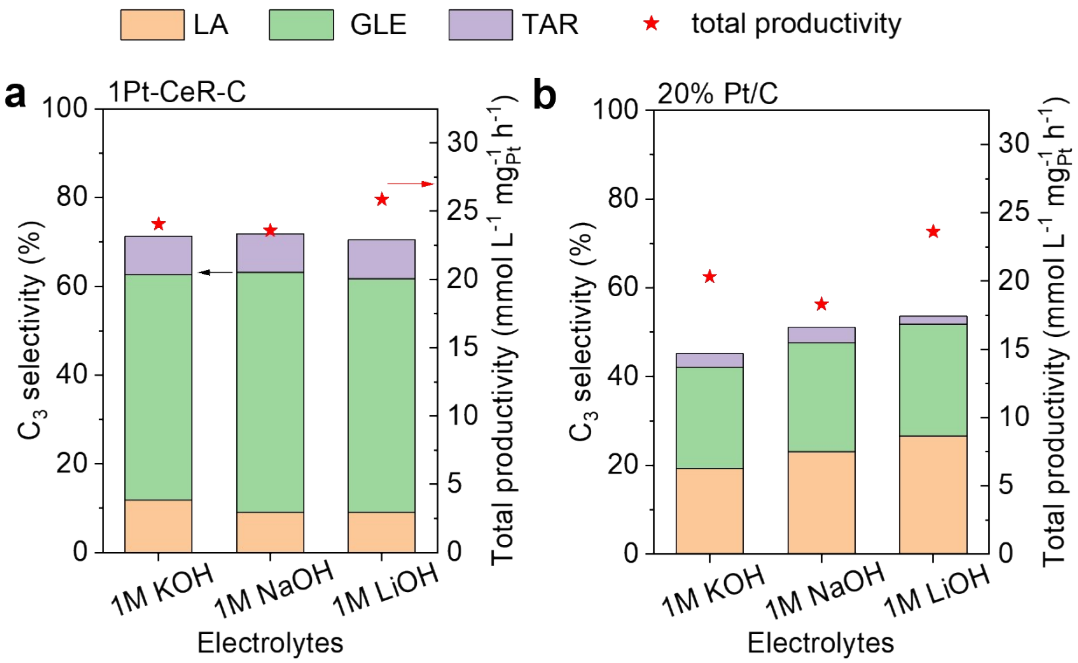

Figure S17. C_3 products selectivity and total productivity of products in different electrolytes with 0.1 M glycerol for a) 1Pt-CeR-C and b) 20% Pt/C at applied potential of 1.0 V_{RHE} for 3 hrs. The solution at pH 7 was prepared using potassium phosphate buffer solution.

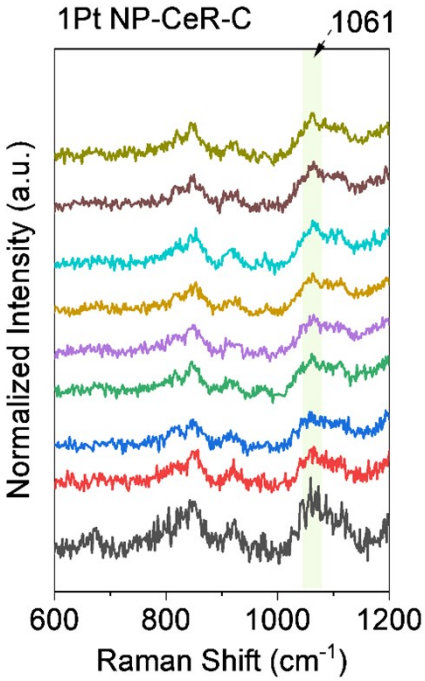

Figure S18. In situ Raman spectra recorded for 1Pt NP-CeR-C at varied potentials in 1 M KOH + 0.5 M glycerol.

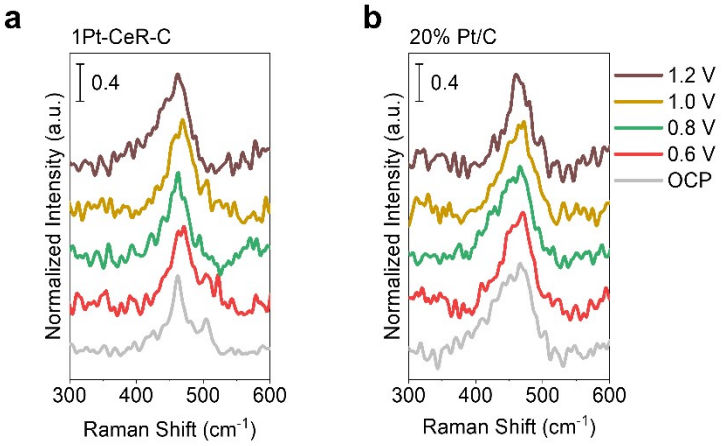

Figure S19. In-situ Raman spectra recorded for a) 1Pt-CeR-C and b) 20% Pt/C at varied potentials in 1 M KOH.

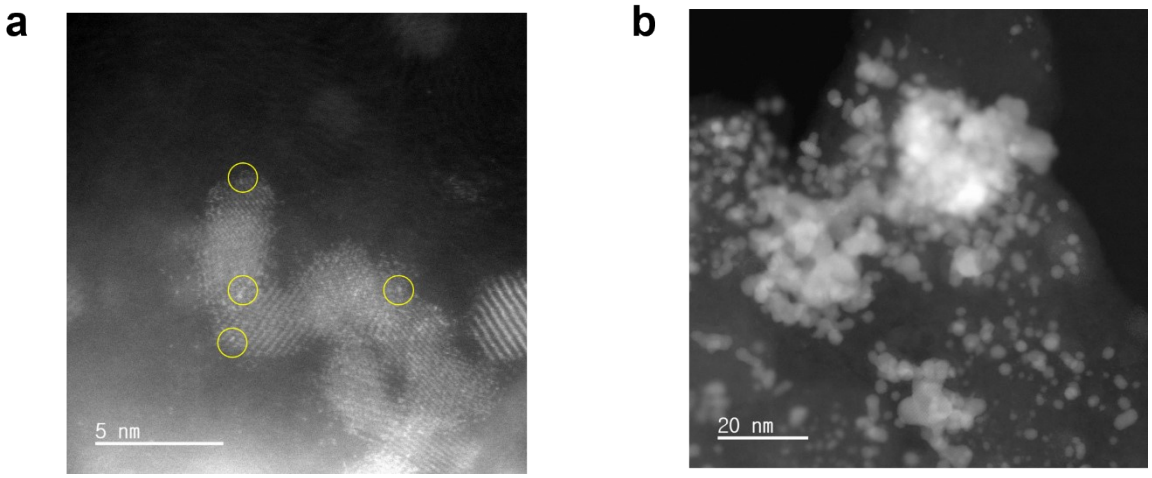

Figure S20. HAADF-STEM images of a) 1Pt-CeR-C and b) 20% Pt/C after the reaction under 1.0 V_{RHE} for 48 hrs.

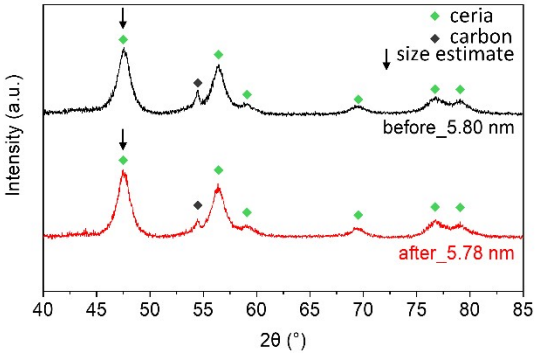

Figure S21. XRD patterns of 1Pt-CeR-C before and after the reaction under 1.0 V_{RHE} for 48 hrs. The black and green diamonds represent carbon and ceria peaks, respectively. The ceria size was estimated from the peak at 47.5° using Scherer's equation.

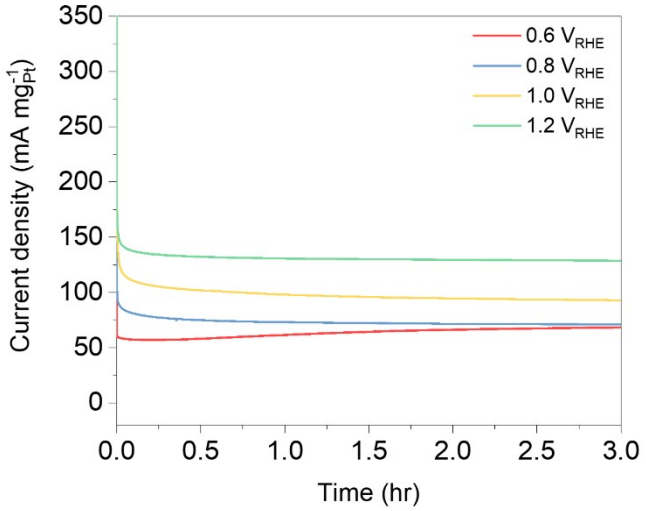

Figure S22. Chronoamperometric curves using the 1 cm^2 flow cell under 0.6 V_{RHE}, 0.8 V_{RHE}, 1.0 V_{RHE}, and 1.2 V_{RHE}, 3 hrs for 1Pt-CeR-C. The current was normalized by Pt mass loading.

Table S3. GEOR productivity, selectivity, glycerol conversion (η_{gly}), and total faradaic efficiency (FE) for 1Pt-CeR-C, using a 1 cm^2 flow cell in an electrolyte of 1 M KOH + 0.1 M glycerol at different potentials.

Catalyst	Potential (V_{RHE})	Productivity (mmol L^{-1} mg_{Pt}^{-1} h^{-1}) (Selectivity (%))						η_{gly} (%)	FE (%)
		LA	GLE	TAR	GLO	ACT	FA		
1Pt-CeR-C	0.6	3.27 (15.5)	9.75 (46.2)	2.26 (10.7)	3.00 (14.2)	1.04 (4.9)	1.78 (8.4)	19.6	95.0
	0.8	4.26 (16.9)	11.65 (46.1)	1.35 (5.3)	3.94 (15.6)	1.17 (4.6)	2.89 (11.4)	21.6	95.8
	1.0	5.10 (15.6)	16.20 (49.6)	1.34 (4.1)	4.71 (14.4)	1.49 (4.6)	3.83 (11.7)	28.1	99.7
	1.2	4.97 (11.6)	21.66 (50.6)	1.06 (2.5)	7.31 (17.1)	1.62 (3.8)	6.15 (14.4)	35.7	100.5

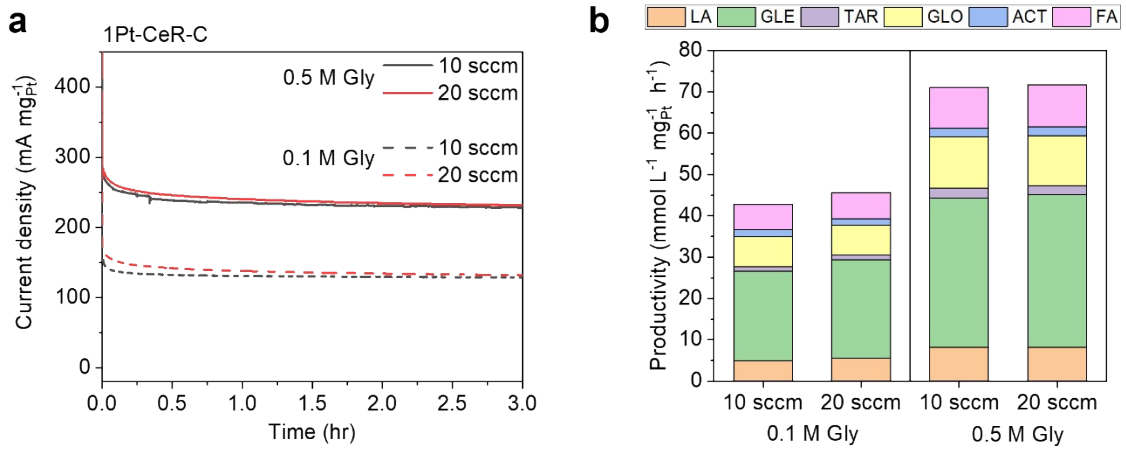

Figure S23. a) Chronoamperometric curve and b) the productivity for GEOR of 1Pt-CeR-C using the 1 cm^2 flow cell when the concentration of electrolyte and its flow rate were varied. 1.2 V_{RHE} was applied during every experiment for 3 hrs.

Table S4. GEOR productivity, selectivity, glycerol conversion (η_{gly}), and total faradaic efficiency (FE) for 1Pt-CeR-C, using a 1 cm^2 flow cell in different electrolytes and flow rates at 1.2 V_{RHE}.

GLY conc	Flow rate (sccm)	Productivity (mmol L^{-1} mg_{Pt}^{-1} h^{-1}) (Selectivity (%))						η_{gly} (%)	FE (%)
		LA	GLE	TAR	GLO	ACT	FA		
0.1 M	10	4.97 (11.6)	21.66 (50.6)	1.06 (2.5)	7.31 (17.1)	1.62 (3.8)	6.15 (14.4)	35.7	100.5
	20	5.58 (12.2)	23.75 (52.0)	1.21 (2.6)	7.16 (15.7)	1.62 (3.5)	6.36 (13.9)	39.2	102.8
0.5 M	10	8.21 (11.5)	36.10 (50.8)	2.37 (3.3)	12.41 (17.5)	2.11 (3.0)	9.90 (13.9)	20.3	99.6
	20	8.13 (11.3)	37.01 (51.6)	2.20 (3.1)	11.96 (16.7)	2.24 (3.1)	10.20 (14.2)	21.4	101.3

Table S5. Comparison of recently reported Pt-based catalysts for glycerol electrooxidation.

Catalyst	Electrolyte[a)]	Condition[b)]	Max. GLE Selectivity	Max. GLE productivity (mmol L^{-1} mg_{PGM}^{-1} h^{-1})	Ref
1Pt-CeR-C	1 M KOH + 0.5 M gly	1.2 V, 3 hrs flow cell	51.6 %	37.0	This work
$Pt_{75}Fe_{25}$/C Polyol	0.1 M NaOH + 0.5 M gly	0.7 V, 4 hrs	79 %	10.0	1
Pt_{cube}	1 M KOH + 0.1 M gly	0.87 V, 2 hrs	40 %	6.65	2
Pt@Pd NPs	0.5 M KOH + 0.5 M gly	0.2V vs SCE, 1 hr	14 %	-	3
PtCu/C	1 M KOH + 0.5 M gly, 60 ℃	1.0 V	45 %	-	4
Hp-PtAu/NF	1 M KOH + 0.5 M gly	1.2 V, 2 hrs	46 %	15.8	5
PtRu/GNS	0.5 M KOH + 0.5 M gly	0.2 V vs SCE, 1 hr	40 %	0.8	6
PC80	2 M KOH + 1 M gly	0.87 V, 2 hrs	34 %	18.7	7
Pt@G	1 M KOH + 0.05 M gly	1.1 V, 4000 s (constant)	27 %	-	8
		0.3-1.1 V, 4000 s (pulse)	39 %	-	
20 wt% Pt-CeO_2/CNT	1 M KOH + 0.1 M gly, 60 ℃	0.9 V, 14 hrs	36 %	-	9

a) Unless noted, temperature is room temperature, b) Unless noted, potential is vs RHE

Table S6. GEOR productivity and selectivity for 1Pt-CeR-C, using a 5 cm^2 flow cell for 100 hr stability test in 1 M KOH + 0.5 M GLY at 1.0 V_{RHE}.

Condition	Time (hr)	Productivity (mmol L^{-1} mg_{Pt}^{-1} h^{-1}) (Selectivity (%))						C_3 selectivity (%)
		LA	GLE	TAR	GLO	ACT	FA	
1 M KOH + 0.5 M GLY, 20 sccm	24	6.17 (9.0)	35.80 (52.2)	1.16 (1.7)	13.57 (19.8)	1.28 (1.9)	10.54 (15.4)	62.9
	48	8.48 (12.4)	36.73 (53.5)	0.83 (1.2)	12.29 (17.9)	0.87 (1.3)	9.45 (13.8)	67.1
	72	9.06 (13.7)	35.25 (53.2)	1.00 (1.5)	11.28 (17.0)	1.28 (1.9)	8.34 (12.6)	68.4
	100	7.07 (11.5)	30.31 (49.1)	1.25 (2.0)	12.43 (20.1)	1.02 (1.7)	9.66 (15.6)	62.6

References

1. V. S. Lima, T. S. Almeida and A. R. De Andrade, *Journal*, 2023, **13**.
2. I. Terekhina and M. Johnsson, *Nanoscale*, 2024, **16**, 13000-13010.
3. Y. Zhou and Y. Shen, *Electrochemistry Communications*, 2018, **90**, 106-110.
4. L. S. Oh, J. Han, E. Lim, W. B. Kim and H. J. Kim, *Journal*, 2023, **13**.
5. Y. Li, X. Wei, R. Pan, Y. Wang, J. Luo, L. Li, L. Chen and J. Shi, *Energy & Environmental Science*, 2024, **17**, 4205-4215.
6. Y. Zhou, Y. Shen and J. Piao, *ChemElectroChem*, 2018, **5**, 1636-1643.
7. I. Terekhina and M. Johnsson, *ACS Applied Materials & Interfaces*, 2024, **16**, 56987-56996.
8. W. Chen, L. Zhang, L. Xu, Y. He, H. Pang, S. Wang and Y. Zou, *Nature Communications*, 2024, **15**, 2420.
9. J. Li, Z. Li, Z. Zheng, X. Zhang, H. Zhang, H. Wei and H. Chu, *ChemCatChem*, 2022, **14**, e202200509.